ON THE MEASUREMENTS BY RADIOMETERSONDE AT SYOWA STATION, ANTARCTICA

Takashi YAMANOUCHI,

National Institute of Polar Research, 9–10, Kaga 1-chome, Itabashi-ku, Tokyo 173

Yuji YAMAMOTO, Shigemi MESHIDA

Japan Meteorological Agency, 3–4, Otemachi 1-chome, Chiyoda-ku, Tokyo 100

and

Akihiro UCHIYAMA

Faculty of Science, Tohoku University, Sendai 980

Abstract: Vertical distributions of radiation components were measured by a radiometersonde flown at Syowa Station in 1979. Verification of the measured radiation flux was done in the case of four clear days by comparing to the calculated flux using the data from a routine radiosonde.

The measured downward flux coincided with the calculated flux in some cases, in other cases, it was rather smaller than the calculated flux. The measured upward flux was always smaller than the calculated flux. The discrepancy amounted to 0.06 ly/min at most. The reasons for the discrepancies of both fluxes are discussed and some are found to be within the uncertainties of the data used in the calculation. However, there still exist some differences, attributed to the errors of the radiometersonde measurements. An example of the seasonal variation of the cooling rate is also shown.

1. Introduction

Measurements of vertical distribution of radiation components were planned under the radiation budget measuring program of POLEX-South (Polar Experiment-South). Details of the program of POLEX-South were given by KUSUNOKI (1981). Radiometersonde observations were made at Syowa Station (69°00′S, 39°35′E) in 1979 by the Japanese Antarctic Research Expedition (JARE).

Lots of measurements by radiometersonde have been made by JARE. About 140 sondes flown at Syowa Station between 1967 and 1969 were analyzed by KAWAGUCHI (1979) and radiation properties of the Antarctic atmosphere were discussed. However, there still existed some uncertainties in the values measured by radiometersonde. GILLE and KUHN (1973) reported the results of intercomparison of radiometersonde observations from several countries. It was shown in the report that

there were some differences between the measured values of respective sondes, and a question remained as to which was the most plausible. KANO and MIYAUCHI (1977) reported the comparison between the longwave flux observed by radiometersonde and the flux obtained by calculation. Discrepancies were found between both of the fluxes, it was concluded that the discrepancies at the lower level were due to aerosols and water vapor continuum absorption, which were not incorporated in the calculations, and those at the upper level were attributed to the measurement errors of the radiometersonde. The problems of the measurement errors were studied by AEROLOGICAL OBSERVATORY (1978), and some improvements of the sensor were proposed. The sensors of the present measurement were of the type which was partly improved according to that proposal. Since that time, no field observations by radiometersonde have been made in Japan; and the observations at Syowa Station are the only results with the present type sonde, and hence are valuable.

In 1979, on account of scarce flight of radiometersonde, it was difficult to discuss the statistical properties of Antarctic atmosphere. The present paper are restricted mainly to the verification of the measured value of radiometersonde by the comparison with the calculated value.

2. Radiation Flux by Radiometersonde

The R-69 type radiometersondes used in the present measurements are composed of two sensors of the same type, one upfacing and the other downfacing. A schematic cross section of the sensor is shown in Fig. 1. From the temperature of

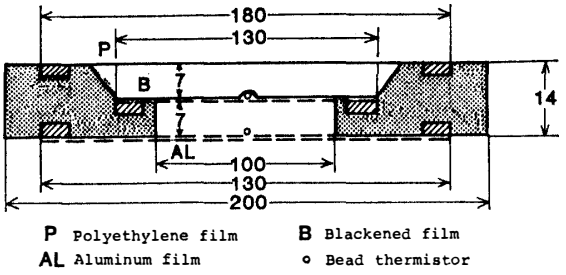

Fig. 1. Schematic cross-section of radiometersonde sensor.

the blackened receiver surface T_r and that of the aluminum film T_s, the radiation flux F is derived as

$$F=\sigma T_r^4+K(T_r^2-T_s^2)+C\frac{dT_r}{dt}\,, \tag{1}$$

where

σ: Stefan-Boltzmann constant,

$$K=\left(\frac{1}{\alpha}+\frac{1}{\tau}-1\right)\frac{k}{d}$$

$$C=\left(\frac{1}{\alpha}+\frac{1}{\tau}-1\right)C_r$$

and

α: absorptivity of blackened surface of receiving film,
τ: transmissivity of polyethylene film,
k: coefficient of proportionality of thermal conductivity
d: distance between the films,
C_r: heat capacity of receiving film.

Details of the derivation of eq. (1) were shown in the reference (GILLE and KUHN, 1973). For the constants K and C, experimentally predetermined values were used.

Mounting of thermistors for the measurement of the temperature of the aluminum film was changed to the inner side from that of the former type, as shown in Fig. 1 according to the proposal by AEROLOGICAL OBSERVATORY (1978). According to that report, the temperature measurement of the aluminum film should be improved by this method.

3. Radiation Flux from the Calculation

Upward and downward longwave fluxes for the wavenumber region r, $F_r\uparrow$ and $F_r\downarrow$, are expressed as

$$\left.\begin{aligned} F_r\uparrow(z)&=T_r(z,0)B_r(g)+\int_0^z B_r(z')\frac{\partial T(z,z')}{\partial z'}\,\mathrm{d}z' \\ F_r\downarrow(z)&=T_r(Z,z)B_r(Z)-\int_z^Z B_r(z')\frac{\partial T(z,z')}{\partial z'}\,\mathrm{d}z' \end{aligned}\right\} \tag{2}$$

where the subscript r denotes the spectral interval, $T(z, z')$ the flux transmission between levels z and z', B the Planck black body flux, Z the upper boundary of the atmosphere for the calculations and $B_r(g)$ is the flux incident on the bottom of the atmosphere ($z=0$) from the ground. Calculations were done using the method of RODGERS and WALSHAW (1966). In estimating the transmission function the Goody random model was used, and as for the angle integration of the flux transmission function, a diffusivity factor of 1.66 was used. If two absorption bands overlapped, the multiplication property was assumed. In order to treat an inhomogeneous atmosphere, the Curtis-Godson approximation was employed, and two parameters, equivalent amount $\bar{m}$ and equivalent pressure $\bar{\phi}$, were introduced.

$$\left.\begin{aligned} \bar{m} &= \int \Phi(\theta)\,\mathrm{d}m\,, \\ \bar{\phi} &= \frac{1}{m}\int \Psi(\theta)\phi\,\mathrm{d}m\,, \end{aligned}\right\} \tag{3}$$

where θ is the temperature, $\phi = P/P_0$ and m is the absorber amount. P denotes the atmospheric pressure and the subscript 0 denotes the standard condition. $\Phi(\theta)$ and $\Psi(\theta)$ of eq. (3) are shown as follows.

$$\left.\begin{aligned} \Phi(\theta) &= \frac{\sum_i k_i(\theta)}{\sum_i k_i(\theta_s)}\,, \\ \Psi(\theta) &= \left[\frac{\sum_i \sqrt{k_i(\theta)\alpha_{i0}(\theta)}}{\sum_i \sqrt{k_i(\theta_s)\alpha_{i0}(\theta_s)}}\right]^2\,, \end{aligned}\right\} \tag{4}$$

where θ_s is a standard temperature (set to 260 K) and k_i and α_i are the line intensity and Lorentz line width of the i-th line. $\Phi(\theta)$ and $\Psi(\theta)$ of eq. (4) were interpolated from the calculated values at several typical temperatures at 25 K intervals.

Actual calculations were done respectively in 140 spectral intervals of 10 to 25 cm^{-1} width. The spectral data used in the calculation were: H_2O rotational band (0–800 cm^{-1}), 6.3 μm band (1200–2200 cm^{-1}), CO_2 15 μm band (520–840 cm^{-1}), 4.3, 4.8 and 5.2 μm bands (1800–2450 cm^{-1}), O_3 rotational band (0–160 cm^{-1}), 14 μm band (610–800 cm^{-1}), 9.6 μm band (950–1180 cm^{-1}) and H_2O continuum absorption (750–1200 cm^{-1}). Line parameters for these absorption bands were derived from the conpilation of AFCRL line parameters by McCLATCHEY *et al.* (1973). For the H_2O continuum, the absorption coefficient k_ν at the wavenumber ν was derived from ROBERTS *et al.* (1976) as follows.

$$k_\nu = k_\nu^0[e + \gamma(P - e)]\,, \tag{5}$$

where k_ν^0 is the absorption coefficient for the standard condition, e and P are the pressures of water vapor and the total atmosphere, respectively, and 0.005 was assumed for γ.

The temperature distribution used in the calculation was obtained from the radiometersonde; however, water vapor was not measured by it. The average value of the water vapor amount used in the calculation was derived from the measurements of the routine radiosondes flown about 6 hours before and after the radiometersonde. However, the measurement of relative humidity was only done up to the 600 or 500 mb level; the water vapor distribution at the upper level was assumed. Above the 70 mb level, the H_2O mixing ratio was given as 2.0×10^{-6} g/g, and between the top of the measured level and the 70 mb level, the mixing ratio was smoothly interpolated as shown in Fig. 2. These estimated values were consistent with the

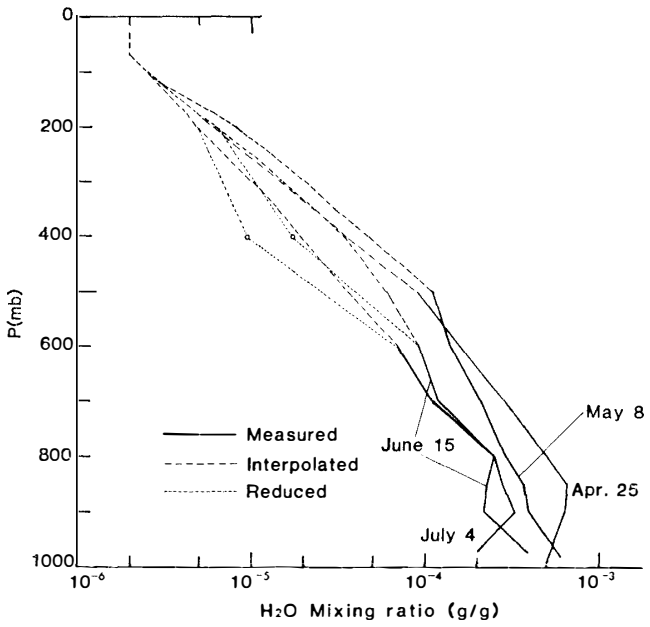

Fig. 2. Water vapor mixing ratio used in the calculations.

mixing ratio measured in the upper atmosphere in mid-latitude by MASTENBROOK (1968). CO_2 was assumed to be distributed uniformly, and the mixing ratio was taken to be 4.86×10^{-4} g/g. For the O_3 distribution, mid-latitude data from KRUGER and MINZNER (1976) were used.

4. Comparison between Measured and Calculated Flux

Among eleven radiometersondes flown in 1979, four sondes were flown on clear days, April 25, May 8, June 15 and July 4. Calculations of flux and divergence were made for these four days, and the results are compared with the measured results in Figs. 3 to 6. Measured fluxes at the standard pressure levels shown in Figs. 3 to 6 were interpolated from the originally measured points. Temperature and water vapor distributions used in the calculation are shown on the left hand sides of these figures. Since it is difficult to interpret the effect of clouds precisely in the calculation, a comparison was not made for the cloudy day.

4.1. Downward flux

In Fig. 3, the measured and calculated downward fluxes show different rates of increase. The calculated flux is smaller than the measured flux at levels higher than 350 mb and lower than 800 mb. The difference at the upper level exceeds 0.02 ly/min, which accounts for a great percentage at the higher level. This discrepancy may be due partly to the fact that the top of the atmosphere was set at around 30 mb in

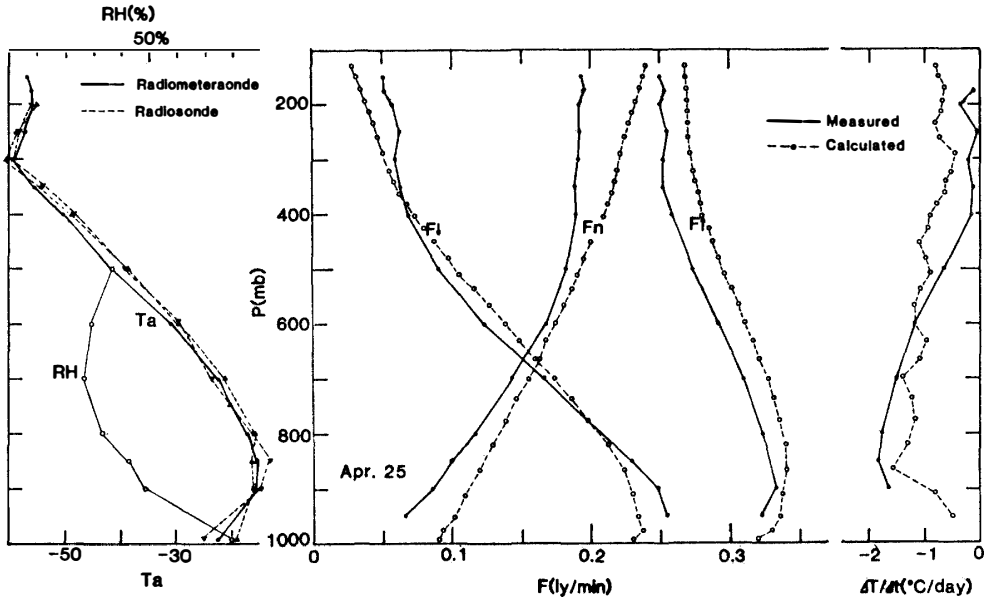

Fig. 3. Measured and calculated radiation flux and cooling rate for April 25, 1979. In the left hand side, temperature and relative humidity.

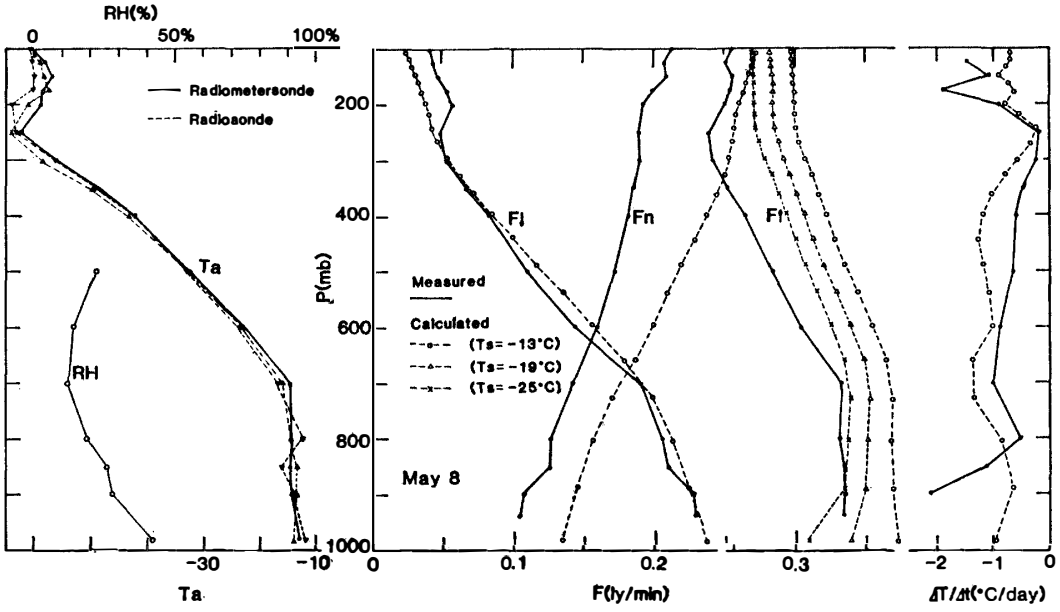

Fig. 4. Same as Fig. 3 but for May 8, 1979.

the calculation, and to the difference in the O_3 contribution in the calculation, since the O_3 distribution of mid-latitude was assumed for that at high latitude. However, the contribution of O_3 to the downward flux was about 0.002 ly/min at 200 mb; the

whole discrepancy cannot be attributed to the difference in the distribution of O_3. Since we have no accurate information about other radiative components, as pointed out by SEKIHARA (1975), the radiation flux at upper levels is still uncertain. Uncertainties of measurement may also exist. Since the calculation error in the present scheme may become large at upper levels, it is not appropriate to make a comparison of the present results above 200 mb. The large discrepancy at the lowest levels is another matter. Though the sky was reported to be clear from synoptic observations, there might have been some clouds at low levels. In general, the measured and calculated fluxes coincide within 10% between 300 and 850 mb level.

In Fig. 4 for May 8, the same kind of discrepancy between measured and calculated fluxes is seen, except in the lowest layer. In the lowest layer, the fluxes agree in this case. As a whole, the measured and calculated flux coincide within 10% below the 250 mb level.

In Figs. 5 and 6 for June 15 and July 4, the measured fluxes are too large in the upper level above 200 mb, but the amounts of excess are not so large as in Figs. 3 and 4. Below the 300 mb level, the calculated flux is much larger than the measured flux in the whole region; the discrepancy has a maximum of about 0.025 ly/min around 500 to 600 mb. Some of the sources of the discrepancy above are water vapor and temperature distributions, since CO_2 is distributed uniformly and the O_3 contribution may not be effective at the low level. At lower levels than 600 mb, the H_2O distribution was derived from the measured value even though it is not always reliable, and at higher levels the H_2O mixing ratio did not seemed to be too high,

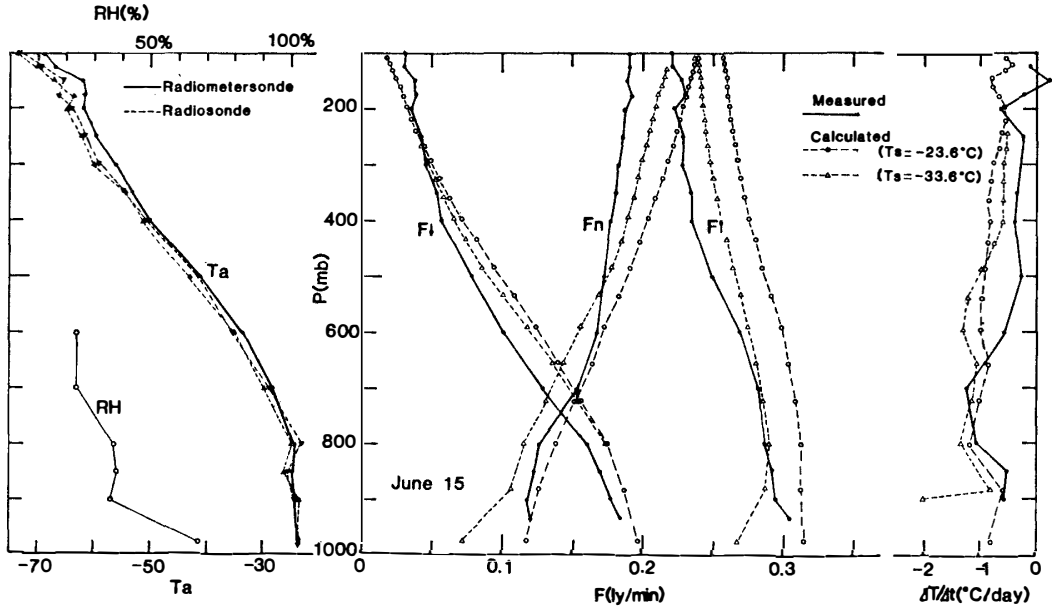

Fig. 5. Same as Fig. 3 but for June 15, 1979. Triangles for the calculated downward flux are for the reduced water vapor amount.

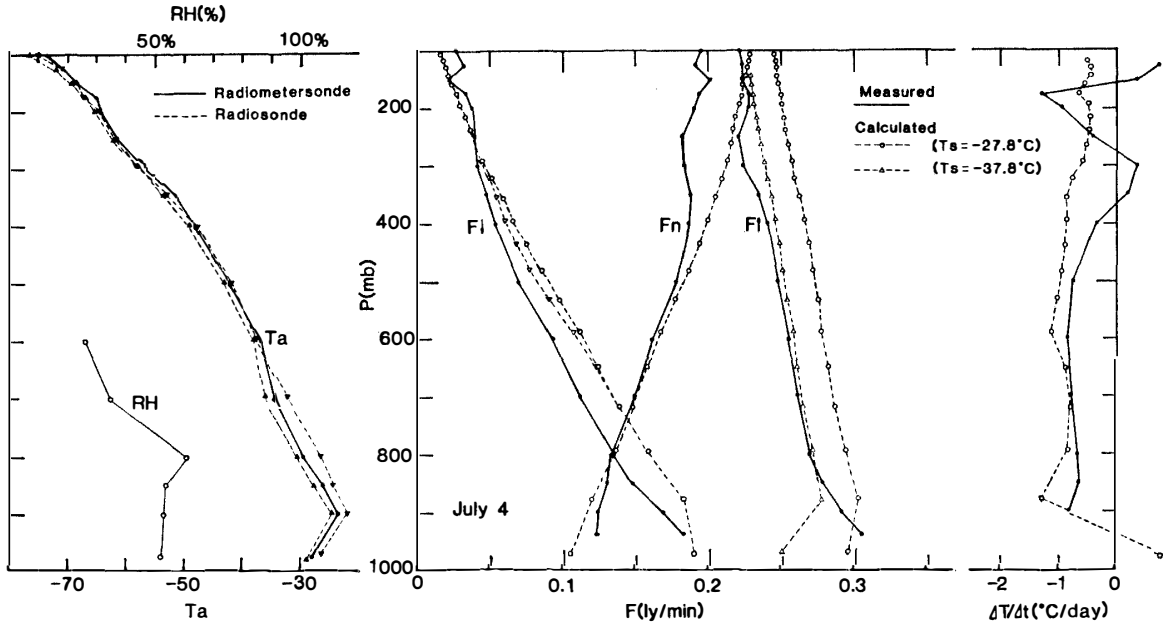

Fig. 6. Same as Fig. 5 but for July 4, 1979.

because the calculated flux was smaller than the measured. Mixing ratios above 200 mb and below 600 mb were fixed, and between 200 and 600 mb were reduced as shown in Fig. 2 by thin dotted lines; the mixing ratio at 400 mb was reduced to half. Using these unsmoothed distributions of water vapor, calculated fluxes are reduced as indicated in Figs. 5 and 6; the reduction amounts only to 0.01 ly/min at most and does not compensate for the whole difference between the calculated and measured fluxes.

As for the temperature distribution, there also exist some uncertainties. In the left-hand side of Fig. 5, temperatures from a routine radiosonde, which are plotted by triangle, are lower for both flights than the temperature from the radiometersonde above 700 mb. It is not certain whether this difference in temperature of about 1 to 3°C is a natural diurnal variation or merely an experimental error. If the temperatures of the whole layer were lowered by 2°C, the downward flux would be reduced by 0.004 ly/min at 300 mb, 0.005 ly/min at 500 mb and 0.009 ly/min at 700 mb, respectively, and would account partly for the difference between the fluxes.

In general, the relation between calculated and measured downward flux below the 300 mb level is reversed from that reported by KANO and MIYAUCHI (1977); their calculated flux was smaller than the measured flux. In their report, the contribution from water vapor continuum absorption and aerosols which were not introduced in their calculation were suggested to be responsible for the difference between the measured and calculated fluxes. But in the present calculation the former was already incorporated, and the latter contribution, which was not incorporated because

its contribution is still uncertain, seemed to be less effective in the Antarctic atmosphere. The difference between sonde sensors used for those observations was in the way of mounting of the thermistor for the measurement of the aluminum film temperature T_s. In the former model, the thermistor was mounted outside the film and was effected by air temperature T_a; however, in the present model, it was mounted inside. With this improvement, T_s would appart from T_a and would approach T_r, while $T_a > T_s > T_r$ for the upfacing sensor. It is assumed from eq. (1) that the downward flux will increase. This tendency varies in the actual measured values.

4.2. Upward flux

In Figs. 3 to 6, the measured fluxes are smaller than the calculated fluxes in all cases, though the differences are not the same. The difference is largest in Fig. 4 for May 8, 0.03 ly/min at 900 mb and a maximum of 0.06 ly/min around the 300 mb level.

One of the reasons for the discrepancy is the difference in ground surface temperature. In the calculation of eq. (2), the surface temperature was assumed to be equal to the air temperature at the lowest level (1.5 m height) because there were no surface temperature data. However, the surface temperature might be lower than the air temperature at 1.5 m, if a strong inversion is formed above the snow surface. From the vertical profiles of temperature, inversions of 4 to 7°C are seen between 900 mb and the lowest level for April 25 and July 4. At Mizuho Station, surface inversions of more than 5°C are frequently seen between the surface and the 2 m level (YAMANOUCHI *et al.*, 1981). In Fig. 4, additional calculated results for the upward flux are presented, with surface temperatures of −19 and −25°C, respectively, in place of the original value of −13°C. In the result for −19°C, the calculated flux at the lowest point seems to agree with the measured flux; however, the former increases more than 0.01 ly/min above 800 mb and the differences between both fluxes are amplified at the upper level. The calculated result for unrealistic surface temperature of −25°C also deviates from the measured flux at upper levels, though the measured flux is larger at the lowest level. Trends of decrease are different for both the fluxes.

For June 15 and July 4, additional calculations of upward flux were also done with regard to the surface temperature 10°C lower than the original lowest level air temperature. Systematic relations between calculated and measured flux are the same in Figs. 5 and 6; however, the difference between the fluxes is larger in Fig. 5 than in Fig. 6 at the higher levels. At the lower levels, measured fluxes are rather greater than the recalculated fluxes, and also greater than the original calculated fluxes for July 4.

Discrepancies between calculated and measured flux cannot be explained merely by the reduction of surface temperature in the calculations as described above. Another possible explanation for the difference between the fluxes is horizontal move-

ment of the radiometersonde to a place of different surface condition and temperature. If the sonde flew gradually to a place of lower temperature, upward flux would decrease more rapidly than the present calculated flux. Though the tendency of the measured flux can be qualitatively explained by this assumption, it is difficult to give a quantitative explanation. As for the actual flight path, if a westerly wind prevailed, the sonde would fly to the slope of the Antarctic Continent (Syowa Station is on an island offshore), and such an explanation as mentioned above could be valid. From the wind direction derived from the routine sonde, a westerly wind was found for April 25 and for the higher level of July 4. For the other days, wind directions were roughly east or north-east, and sondes were expected to flow on to the sea ice, as that surface and atmospheric temperatures would not be expected to be low enough to explain the difference between the measured and calculated fluxes. As for the sources of calculations, judging from the difference between calculated and measured flux, larger amounts of absorber are preferable. However, from Subsection 4.1, the results are rather to the contrary.

Consequently, there may remain uncertainties in the measured values for the upward flux.

4.3. Net flux and divergence

A comparison between measured and calculated net fluxes is given here, though it may have less physical meaning on account of large discrepancies in the downward and upward fluxes, respectively. In order to obtain a cooling rate—divergence—an absolute value of net flux is not necessary. In Figs. 3 to 6, absolute values of calculated and measured net flux vary; however, the slopes of both fluxes are similar at the lower levels below 500 or 600 mb. This reflects the trends of the cooling rate which are shown on the right hand sides of Figs. 3 to 6. Vertical distributions of cooling rate are roughly simulated by calculation between 600 and 900 mb. At upper levels discrepancies between the measured and calculated cooling rates are quite large, as a consequence of discrepancies in the upward and downward fluxes, respectively. The measured cooling rates indicated in the figures are the smoothed values derived from the net flux at the standard pressure level. The cooling rate derived from the net flux at measured level shows large variation and is unreliable.

For June 15, another calculation of net flux and divergence was done for reduced water vapor and reduced surface temperature, and indicated with white triangle. The cooling rate by this calculation does not seem to be much improved.

5. General Features of the Cooling Rate

Though there remain large discrepancies in the measured cooling rate, the vertical profile of which resembles the calculated cooling rate to some extent, and it is worth while to examine the seasonal variation of the atmospheric radiative cool-

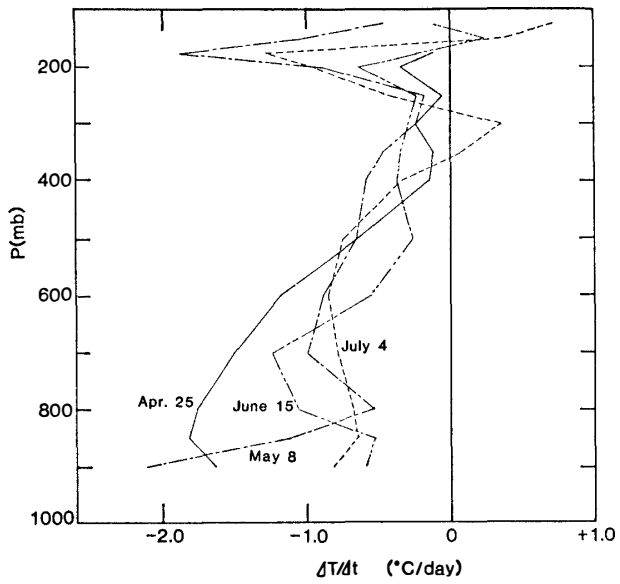

Fig. 7. Comparison of cooling rates from four flights of the radiometersonde.

ing. In Fig. 7, the vertical distributions of measured cooling rates are compared together, just as on the right-hand sides of Figs. 3 to 6. As an example, in Fig. 7, below the 250 mb level, the seasonal variation of the cooling rate is such that the level of the maximum cooling rate goes upward according to the advance of the season. This seasonal trend of cooling rate is similar to that reported by KAWAGUCHI (1979). From his report, the maximum cooling rate occurred around 700 and 800 mb in winter, and which occurred lower in April.

The average cooling rates of the total layer between 250 and 950 mb were derived as −1.02, −0.86, −0.63 and −0.55°C/day for April 25, May 8, June 15 and July 4, respectively. Cooling rates gradually decrease toward winter; however, air temperature is rather higher for May 8 than for April 25.

6. Concluding Remarks

It is difficult to conclude about the reliability of measured radiation flux on account of several uncertainties in the data adopted in the calculation.

The measured downward fluxes are reasonable in the lower layer below 500 or 600 mb, where the data of the H_2O distribution are available, though only gradients for June 15 and July 4. Between 200 and 600 mb, calculations are variable according to the distribution of H_2O and temperature. Above 200 mb, it is not appropriate to assess the measured downward flux from the present calculation. As for upward flux, there is a large discrepancy between the measured and calculated fluxes. Though some correction and variation of surface temperature in the calculation were con-

sidered, the whole discrepancy between measured and calculated cannot be explained thoroughly. Also, some uncertainties in the measured flux attributed to the radiometersonde sensor are expected.

Several problems are presumed to exist with the method of temperature measurement of the receiving film and reflecting aluminum film, on the distortion of the polyethylene and aluminum film and on the constants K and C of eq. (1). However, it is imposible to clarify the problem which influences the measurement most from the present study.

In order to make a precise verification, simultaneous observations by radiometersonde and of water vapor distribution—one possible method is a dew point sonde—should be made. Another experiment for the calibration of the sensor should also be done.

Acknowledgments

The authors wish to express their sincere thanks to the members of the meteorological party of JARE-20, Mr. K. TSUKAMURA and Mr. M. KOSHA of the Japan Meteorological Agency, for their support to the observations. Special thanks are due to Dr. M. KANO and Mr. M. MIYAUCHI, Meteorological Research Institute, for their kind advice in the analysis of data. Thanks are also due to Prof. S. KAWAGUCHI of the National Institute of Polar Research to give one of the authors (T. YAMANOUCHI) the opportunity to do a radiometersonde study in the Antarctic. The authors are indebted to Ms. K. SUKENO for her assistance in preparing the manuscript.

Calculations of radiation flux were done with the aid of the ACOS-900 electronic computer at Tohoku University.

References

AEROLOGICAL OBSERVATORY (1978): Genyô fukusha zonde no kairyô ni tsuite (On the improvement of longwave radiometer sonde used in JMA). Kôsôkishôdai Ihô (J. Aerological Observatory), **39**, 29–40.

GILLE, J. G. and KUHN, P. M. (1973): The International Radiometersonde Intercomparison Programme (1970–1971). Geneva, WMO, 127 p. (WMO Tech. Note, **128**).

KANO, M. and MIYAUCHI, M. (1977): On the comparison between the observed vertical profiles of longwave radiative fluxes and the computed ones in Japan. Pap. Meteorol. Geophys., **28**, 1–8.

KAWAGUCHI, S. (1979): Nankyoku taiki no hôsha tokusei (Radiation properties of Antarctic atmosphere). Doctoral Thesis, Tohoku University, 179 p.

KRUEGER, A. J. and MINZNER, R. A. (1976): A mid-latitude ozone model for the 1976 U.S. standard atmosphere. J. Geophys. Res., **81**, 4477–4481.

KUSUNOKI, K. (1981): Japanese Polar Experiment (POLEX) in the Antarctic in 1978–1982. Mem. Natl Inst. Polar Res., Spec. Issue, **19**, 1–7.

MASTENBROOK, H. J. (1968): Water vapor distribution in the stratosphere and high troposphere. J. Atmos. Sci., **25**, 299–311.

McCLATCHEY, J. N., BENEDICT, W. S., CLOUGH, S. A., BURCH, D. E., CALFEE, R. F., FOX, K., ROTHMAN, I. S. and GARING, J. S. (1973): Atmospheric absorption line-parameters compilation. AFCRL-TR-73-0096, Environ. Res. Pap., **434**, 78 p.

ROBERTS, R. E., SELBY, J. E. A. and BIBERMAN, L. M. (1976): Infrared continuum absorption by atmospheric water vapor in the 8–12 m window. Appl. Opt., **15**, 2085–2090.

RODGERS, C. D. and WALSHAW, C. D. (1966): The computation of infra-red cooling rate in planetary atmospheres. Q. J. R. Meteorol. Soc., **92**, 67–92.

SEKIHARA, K. (1975): A study of radiometer sonde observations of the lower stratosphere in Japan. Pap. Meteorol. Geophys., **26**, 93–110.

YAMANOUCHI, T., WADA, M., MAE, S., KAWAGUCHI, S. and TSUKAMURA, K. (1981): Measurements of radiation components at Mizuho Station, East Antarctica in 1979. Mem. Natl Inst. Polar Res., Spec. Issue., **19**, 27–39.

(*Received April 30, 1981; Revised manuscript received June 5, 1981*)